Single-Walled Carbon Nanotubes: Efficient Nanomaterials for Separation and On-Board Vehicle Storage of Hydrogen and Methane Mixture at Room Temperature?

Piotr Kowalczyk,[†,‡] Lorenzo Brualla,[§] Andrzej Żywociński,[†] and Suresh K. Bhatia*[,‡]

Department III, Soft Condensed Matter, Institute of Physical Chemistry of the Polish Academy of Sciences, 01-224 Warsaw, Poland, Facultat de Física (ECM), Universitat de Barcelona, Diagonal 647, 08028 Barcelona, Spain, and Division of Chemical Engineering, The University of Queensland, Brisbane, Queensland 4072, Australia

Received: December 11, 2006; In Final Form: February 2, 2007

We investigate possible usage of single-walled carbon nanotubes (SWNTs) as an efficient storage and separation device of hydrogen−methane mixtures at room temperature. The study has been done using Grand Canonical Monte Carlo simulations for modeling storage and separation of hydrogen−methane mixtures in idealized SWNTs bundles. These mixtures have been studied at several pressures, up to 12 MPa. We have found that the values of the stored volumetric energy and equilibrium selectivity greatly depend on the chiral vector (i.e., pore diameter) of the nanotubes. The bundle formed by [5,4] SWNTs (nanotube diameter of 6.2 Å) can be regarded as a threshold value. Below that value the densification of hydrogen or methane is negligible. Bundles with wider nanotube diameter (i.e., 12.2, 13.6, 24.4 Å) seem to be promising nanomaterials for hydrogen−methane storage and separation at 293 K. SWNTs with pore diameters greater than 24.4 Å (i.e., [18,18]) are less efficient for both on-board vehicle energy storage and separation of hydrogen−methane mixture at 293 K with pressures up to 12 MPa. SWNTs comprised of cylindrical pores of 8.2 and 6.8 Å in diameter (equivalent chiral vector [6,6] and [5,5], respectively) are the most promising for separation of the hydrogen−methane mixture at room temperature, with the former selectively adsorbing methane and the latter selectively adsorbing hydrogen. We observed that inside the pores of [6,6] nanotubes absorbed methane forms a quasi-one-dimensional crystal when the system has thermalized. The average intermolecular distance of such a crystal is smaller than the one of liquid methane in bulk at 111.5 K, therefore exhibiting the quasi-one-dimensional system clear compression characteristics. On the other hand, for a smaller nanotube diameter of 6.8 Å the hydrogen can enter into the tubes and methane remaining in bulk. We found that in the interior of [5,5] nanotubes adsorbed/compressed hydrogen forms a quasi-one-dimensional crystal.

Introduction

Nanoporous carbonaceous materials are convenient "hosts"—that is, they are useful for storing, separating, and investigating various quest molecules under strong confinement.[1−4] Novel carbon-based nanomaterials, such as single-walled carbon nanotubes (SWNTs), worm-like SWNTs, double-walled carbon nanotubes (DWNTs), single-walled carbon nanohorns (SWNHs), stacked-cup carbon nanofibers (SCCNT), doped fullerenes, wormlike graphitic carbon nanofibers, bamboo-type multiwalled carbon nanotubes, and ordered porous carbons have been regarded as promising media for efficient reversible storage and separation of chemical species.[5−12] Given a hosting carbonaceous material with sufficiently small and uniform nanopores, for example, a bundle of SWNTs, fluid mixtures, exhibiting either a classical or quantum character, can be efficiently separated.[13−20] This separation process results from confinement of molecules in the strong external potential field generated by the walls of the host nanomaterial. For adsorbed fluids, these additional external forces disturb their structure in the near-wall layer of a thickness comparable to a bulk correlation length. Consequently, for adsorbed fluids confinement plays a significant role when the size of the fluid system is up to $10\sigma_{ff}$ (σ_{ff} denotes collision diameter of fluid molecule).[21−23]

SWNT bundles seem to be particularly suitable for on-board vessel fuel storage, separation of chemical species, and detection of guest molecules. They are uniform, well-defined, lightweight, chemically inert, thermally stable, mechanically strong, and environmentally friendly.[24−27] Furthermore, they are suitable for studying quasi-one-dimensional fluids under strong confinement (e.g., compression/expansion and spacing of guest molecules, solvation forces, nucleation barrier, elastic deformation of surface during adsorption/desorption processes, fast transport of guest molecules, equilibrium/dynamics selectivity).[28−36]

In the current paper we investigate the adsorption and separation of hydrogen−methane mixture in idealized bundles of SWNTs at 293 K and pressures from 0.001 Pa up to 12 MPa. The importance of the hydrogen−methane (hythane) separation becomes evident when the main industrial process for hydrogen production for fuel cells is taken into account.[37,38] Coal gas obtained in the destructive distillation of soft coal is primarily composed of hydrogen and methane with small amounts of other hydrocarbons, carbon monoxide, carbon dioxide, and nitrogen.

* Author to whom correspondence should be addressed: e-mail, s.bhatia@eng.uq.edu.au; tel, +61 7 3365 4263; fax, +61 7 3365 4199.
† Department III, Soft Condensed Matter, Institute of Physical Chemistry of the Polish Academy of Sciences.
‡ Division of Chemical Engineering, The University of Queensland.
§ Facultat de Física (ECM), Universitat de Barcelona.

10.1021/jp068484u CCC: $37.00 © 2007 American Chemical Society
Published on Web 03/13/2007

The purification of synthetic gas obtained from steam reforming of natural gas is an important process since 95% of hydrogen used in fuel cells is now produced by this method. Lightweight membranes composed of SWNTs seem suitable for separation of hydrogen or methane from the coal gas mixture.

Hydrogen storage is another issue that has great economic importance and that has triggered many controversial papers. In the light of the recent growing interest on hydrogen, methane, and hythane combustion on vehicles, the on-board storage of these supercritical fluids near ambient temperature is a difficult problem to solve.[39−42] In order to employ methane, hydrogen, or hythane fuel as an alternative to traditional fussy ones, it is necessary to be able to transport them in an economically suitable way. A new generation of ship-tankers could consist of vessels with physisorbed hydrogen that would fulfill the growing demand of hythane in markets such as Asia that cannot be completely satisfied with pipeline distribution.

Further to emerging technological applications, SWNTs provide a new field for exploring the properties of quasi-one-dimensional crystals formed during compression/expansion of adsorbed molecules in the interior space of the individual tubes, and in the interstitial channels among nanotubes in a bundle.[43−47] In this paper we have used Grand Canonical Monte Carlo (GCMC) in order to observe crystal structures that would be not be observed if using any mean-field density functional theory.

This paper is structured in the following way. In the next section we briefly describe the molecular model of the hydrogen−methane mixture adsorption in idealized bundles of SWNTs used in our simulation study at 293 K and pressures ranging from 0.001 Pa up to 12 MPa. Additionally, we define all quantities adopted for the investigation of the efficiency of both energy storage and equilibrium selectivity. The subsequent section presents computational results with discussion. Finally we give conclusions.

Simulation Methods

a. Fluid−Fluid Interaction Potential. We have modeled the methane−methane interactions via the effective truncated central Lennard-Jones potential

$$V_{\mathrm{ff}}^{\mathrm{m}} = 4\epsilon_{\mathrm{ff}}^{\mathrm{m}}\left[\left(\frac{\sigma_{\mathrm{ff}}^{\mathrm{m}}}{r}\right)^{12} - \left(\frac{\sigma_{\mathrm{ff}}^{\mathrm{m}}}{r}\right)^{6}\right]\Theta(r_{\mathrm{cut}} - r) \qquad (1)$$

where r is the distance between two interacting fluid molecules, $\sigma_{\mathrm{ff}}^{\mathrm{m}}$ denotes Lennard-Jones collision diameter, $\epsilon_{\mathrm{ff}}^{\mathrm{m}}$ is the Lennard-Jones well depth, $r_{\mathrm{cut}} = 5\sigma_{\mathrm{ff}}^{\mathrm{m}}$ is the cutoff distance, and Θ stands for the Heaviside function. The Lennard-Jones parameters for methane interactions, $\sigma_{\mathrm{ff}}^{\mathrm{m}} = 3.81$ Å and $\epsilon_{\mathrm{ff}}^{\mathrm{m}}/k_{\mathrm{b}} = 148.12$ K (with k_{b} Boltzmann's constant), were taken from previous studies.[5,14] This potential with parameters given above has been shown to correctly describe the experimental equation of state near ambient temperature.[5]

Following Sese,[48−51] Kowalczyk[42] et al., Levesque[52] et al., and Tanaka[44] et al., we assumed that the hydrogen molecules interact via the quadratic Feynman−Hibbs quantum effective potential

$$V_{\mathrm{ff}}^{\mathrm{H}}(r) = V_{\mathrm{LJ}}(r) + \frac{\beta\hbar^2}{24\mu_{\mathrm{m}}}\left[\frac{\mathrm{d}^2}{\mathrm{d}r^2}V_{\mathrm{LJ}}(r) + \frac{2}{r}\frac{\mathrm{d}}{\mathrm{d}r}V_{\mathrm{LJ}}(r)\right] \qquad (2)$$

where the classical potential $V_{\mathrm{LJ}}(r)$ is represented by a central Lennard-Jones potential, similar to that in eq 1, with different parameters. Here, $\beta = (k_{\mathrm{b}}T)^{-1}$, $\hbar = h/2\pi$ (Planck's constant), and $\mu_{\mathrm{m}} = m/2$ is the reduced mass of a pair of interacting hydrogen molecules. For the hydrogen $V_{\mathrm{LJ}}(r)$ potential we used the parameters $\sigma_{\mathrm{ff}}^{\mathrm{H}} = 2.958$ Å and $\epsilon_{\mathrm{ff}}^{\mathrm{H}}/k_{\mathrm{b}} = 36.7$ K. The second term on the right-hand side of eq 2 accounts for quantum corrections to the statistical properties generated by the classical Lennard-Jones potential. It is noted that near ambient temperature the quantum corrections in the bulk hydrogen can be neglected. The approximation of the diatomic hydrogen molecule by an effective Lennard-Jones potential is justified by the high temperature and low-density region investigated in the current study. In a previous study[42] we showed that the effective second-order Feynman−Hibbs or simple Lennard-Jones potential with parameters given above correctly describes the experimental bulk equation of state.

Hydrogen−methane interactions were modeled according to eqs 1 and 2, with μ representing the reduced quantum mass of the interacting molecules. Hydrogen/methane Lennard-Jones parameters were obtained from the commonly used Lorentz−Berthelot mixing rules: $\sigma_{\mathrm{ff}}^{\mathrm{H-m}} = (\sigma_{\mathrm{ff}}^{\mathrm{H}} + \sigma_{\mathrm{ff}}^{\mathrm{m}})/2$, $\epsilon_{\mathrm{ff}}^{\mathrm{H-m}} = [(\epsilon_{\mathrm{ff}}^{\mathrm{H}}/k_{\mathrm{b}})(\epsilon_{\mathrm{ff}}^{\mathrm{m}}/k_{\mathrm{b}})]^{1/2}$.[53]

b. Solid−Fluid Interaction Potential. SWNTs are naturally obtained in bundles that are stabilized by the van der Walls forces between the individual single carbon nanotubes. As previously,[5] we modeled this ordered carbon nanomaterial by infinitely long idealized hexagonal bundle of SWNTs. Similarly to Steele[54] et al. and Kowalczyk[5] et al. we adopted the structureless model of the individual straight tubes as the basic element of the bundle structure. This assumption is realistic for high temperatures due to the high thermal energy of molecules. Moreover, this approximation is acceptable since the fluid molecule is large relative to the spacing between the surface atoms ($d_{\mathrm{l}}/\sigma_{\mathrm{ff}}^{\mathrm{m}} = 0.37$, where $d_{\mathrm{l}} = 1.42$ Å denotes C−C distance in graphite). Gordillo[55] showed that the presence of a carbon vacancy is enough, at least in some cases, to impede the adsorption of quantum gases in the interstices of a bundle of [10,10] SWNTs. This argument seems to be important if we take into account that even highly purified bundles of SWNTs have impurities inside them (i.e., catalysis, amorphous carbon, etc.) and defects on the pore wall. On the other hand, Iijima[27] et al. synthesized single-walled carbon nanohorns (SWNHs) of purity (>95%). Such a high purity of SWNHs is due to synthesis condition, i.e., CO_2 laser ablation of graphite under argon gas flow at 760 Torr without metallic catalysis. The X-ray diffraction study showed that the interhorn−wall distance is 4 Å, being greater than the interlayer spacing of graphite (3.35 Å).[56,57] Concluding, our idealized model of carbonaceous tubular bundles captured the main properties of the real SWNHs and high-purity bundle of SWNTs. As in our previous study,[5] we assumed that the surface density of carbon atoms smeared on the wall of the carbon tube is $\rho_{\mathrm{s}} = 0.382$ Å^{-2} (i.e., the same as in graphite). The center of the individual structureless carbon tube has coordinates $(x_{\mathrm{c}},y_{\mathrm{c}},z_{\mathrm{c}})$, whereas the radius is defined by R. Additionally, we defined the position of the fluid molecule inside/outside the infinitely long structureless tube by following coordinates $(x_{\mathrm{w}},y_{\mathrm{w}},z_{\mathrm{w}})$, while a point on the carbon surface has coordinates $(x_{\mathrm{p}},y_{\mathrm{p}},z_{\mathrm{p}})$. According to the second-order Feynman−Hibbs[58] effective potential, the total solid−fluid interaction potential can be defined as follows

$$V_{\mathrm{sf}}(R) = 4\epsilon_{\mathrm{sf}}\rho_{\mathrm{s}}R\int_{z_{\mathrm{w}}-ML}^{z_{\mathrm{w}}+ML}\sqrt{1+\left(b\frac{2\pi}{L}\right)^2\cos^2\left(2\pi\frac{z_{\mathrm{p}}}{L}\right)}\,[I_1\sigma_{\mathrm{sf}}^{12} - I_2\sigma_{\mathrm{sf}}^{6} + I_3\psi\sigma_{\mathrm{sf}}^{14} - I_4\psi(1.0/4.4)\sigma_{\mathrm{sf}}^{8}]\,\mathrm{d}z_{\mathrm{p}} \qquad (3)$$

where

$$I_1 = \frac{\pi}{16(a+b)^5\sqrt{a^2-b^2}}\left[\frac{945}{120} + \frac{105}{24}\left(\frac{a+b}{a-b}\right) + \frac{45}{12}\left(\frac{a+b}{a-b}\right)^2 + \frac{45}{12}\left(\frac{a+b}{a-b}\right)^3 + \frac{105}{24}\left(\frac{a+b}{a-b}\right)^4 + \frac{945}{120}\left(\frac{a+b}{a-b}\right)^5\right] \quad (4)$$

$$I_2 = \frac{\pi}{2(a+b)^2\sqrt{a^2-b^2}}\left[\frac{3}{2} + \left(\frac{a+b}{a-b}\right) + \frac{3}{2}\left(\frac{a+b}{a-b}\right)^2\right] \quad (5)$$

$$I_3 = \frac{\pi}{32(a+b)^6\sqrt{a^2-b^2}}\left[\frac{10395}{720} + \frac{945}{120}\left(\frac{a+b}{a-b}\right) + \frac{315}{48}\left(\frac{a+b}{a-b}\right)^2 + \frac{225}{36}\left(\frac{a+b}{a-b}\right)^3 + \frac{315}{48}\left(\frac{a+b}{a-b}\right)^4 + \frac{945}{120}\left(\frac{a+b}{a-b}\right)^5 + \frac{10395}{720}\left(\frac{a+b}{a-b}\right)^6\right] \quad (6)$$

$$I_4 = \frac{\pi}{4(a+b)^3\sqrt{a^2-b^2}}\left[\frac{15}{6} + \frac{3}{2}\left(\frac{a+b}{a-b}\right) + \frac{3}{2}\left(\frac{a+b}{a-b}\right)^2 + \frac{15}{6}\left(\frac{a+b}{a-b}\right)^3\right] \quad (7)$$

$$a = R^2 + \rho^2 + (z_p - z_w)^2 \quad (8)$$

$$b = -2R\rho$$

$$\rho = \sqrt{(x_w - x_c)^2 + (y_w - y_c)^2}$$

$$\psi = \frac{132}{\sigma_{sf}^2}\frac{\beta\hbar^2}{24\mu}$$

In the above equations $L = 10\sigma_{ff}^m$ denotes the length of the basic periodic unit, whereas M is the number of the periodic units used for the calculations of the solid−fluid interaction potential. We have found that $M = 10$ is large enough for the calculation of the total solid−fluid interaction potential in infinitely long structureless single-walled nanotubes owing to fast decreasing of the dispersion interactions.[5] The parameters of the solid−fluid potential (i.e., Lennard-Jones solid−fluid collision diameter (σ_{sf}) and well depth (ϵ_{sf})) were calculated according to the Lorentz−Berthelot mixing rule: $\sigma_{sf}^{x-C} = (\sigma_{ff}^x + \sigma_{ss}^C)/2$, $\epsilon_{sf}^{x-C} = [(\epsilon_{ff}^x/k_b)(\epsilon_{ss}^C/k_b)]^{1/2}$, $\sigma_{ss}^C = 3.4$ Å, and $\epsilon_{ss}^C/k_b = 28$ K, and subscript x denotes methane or hydrogen.[53,14] For methane−tube interactions the quantum corrections terms (i.e., I_3 and I_4 in eq 3) can be neglected owing to a large mass of methane molecules. However, for molecular hydrogen we accounted for both classical and quantum terms in eq 3 since we investigated the pores of molecular size. As pointed out by Wang and Johnson,[59] quantum effects in carbon nanospaces can be important even at 293 K.

c. Simulation Details. In the present work we performed simulations of hydrogen and methane mixture adsorption at 293 K, while bulk mixture pressures ranged from 0.001 Pa up to 12 MPa. We computed the excess part of the chemical potential and partial pressures of the hydrogen−methane mixture in standard canonical ensemble.[53]

In the simulations of hydrogen and methane mixtures in idealized bundles of SWNTs, we used grand canonical ensemble (i.e., fixed system volume, temperature, and chemical potential of the bulk fluid mixture).[53,60] For perturbation of the configuration in GCMC, we selected hydrogen or methane molecules with equal probability. Equal probabilities were used for trial moves, creation, and destruction of the selected molecule, and the acceptance decision followed the Metropolis sampling scheme. In the cubic simulation box we placed an idealized hexagonal bundle of SWNTs consisting of 11 rigid tubes, as displayed in Figures 5−7. Following Tanaka[44] et al., Johnson[59] et al., Levesque[52] et al., Kowalczyk[5] et al., and experimental reports, we used a van der Waals gap of 3.5−4 Å between the individual SWNTs. A cubic simulation box of size $m \times n \times 10\sigma_{ff}^m$ ($\sigma_{ff}^m = 3.81$ Å, n and m values were adjusted according to the assumed intertube distance) with periodic boundary conditions in all directions was used, with the minimum image convention used for computation of molecular interactions. The grand canonical ensemble simulations utilized 1×10^8 configurations, of which the first 6×10^7 were discarded in order to reach equilibrium. The stability of the results was confirmed by additional longer runs of 1.6×10^8 configurations, with the equilibrium composition of hydrogen and methane mixture in idealized bundles of SWNTs fully reproducible.

d. Storage Efficiency and Equilibrium Selectivity. As in our previous study we computed absolute values of adsorption from[5,14]

$$\Omega = \Gamma_H(-\Delta H_H) + \Gamma_m(-\Delta H_m) \quad (9)$$

Here, ΔH_H and ΔH_m denote the heat of hydrogen and methane combustion, respectively. Γ_H and Γ_m denote the absolute value of hydrogen and methane adsorption, respectively. The previous equation states that the heat of reaction per mole equates to the difference in enthalpy of the products and the reactants. Following Dell and Rand,[25] the methane heat of combustion is taken as −55.6 MJ/kg. For hydrogen, the heat of combustion equates to the heat of formation of the product water, i.e., −285.83 kJ/mol of water (−141.789 MJ/kg).[25]

The hydrogen content in the adsorbed phase is critical for the composition of hythane fuel. According to experimental reports the content of hydrogen in hythane fuel should be ≅6−7% by energy.[61,62] Since SWNTs seem to be an attractive storage medium for hythane fuel, we computed the content of hydrogen by energy in the adsorbed hydrogen and methane mixture from

$$\Psi[\%] = 100\,\frac{\Gamma_H(-\Delta H_H)}{\Omega} \quad (10)$$

As mentioned above, the separation of hydrogen and methane mixture at ambient temperature and low pressures is an important technological issue. The primary quantity of interest for separation efficiency is the selectivity. Equilibrium selectivity of methane over hydrogen represents the ratio of the density of these two species in a porous material to the ratio of the density in the bulk phase[63]

$$S = \frac{\rho_m^p/\rho_H^p}{\rho_m^b/\rho_H^b} \quad (11)$$

where ρ_i^p and ρ_i^b are the average density of species "i" in the porous system and bulk phase, respectively. Values grater than unity imply that methane is preferentially adsorbed compared to hydrogen; in contrast, if the selectivity is smaller than unity, hydrogen is preferentially adsorbed.

Results and Discussion

We consider the storage of an equimolar mixture of hydrogen and methane in idealized bundles of SWNTs. The value of the

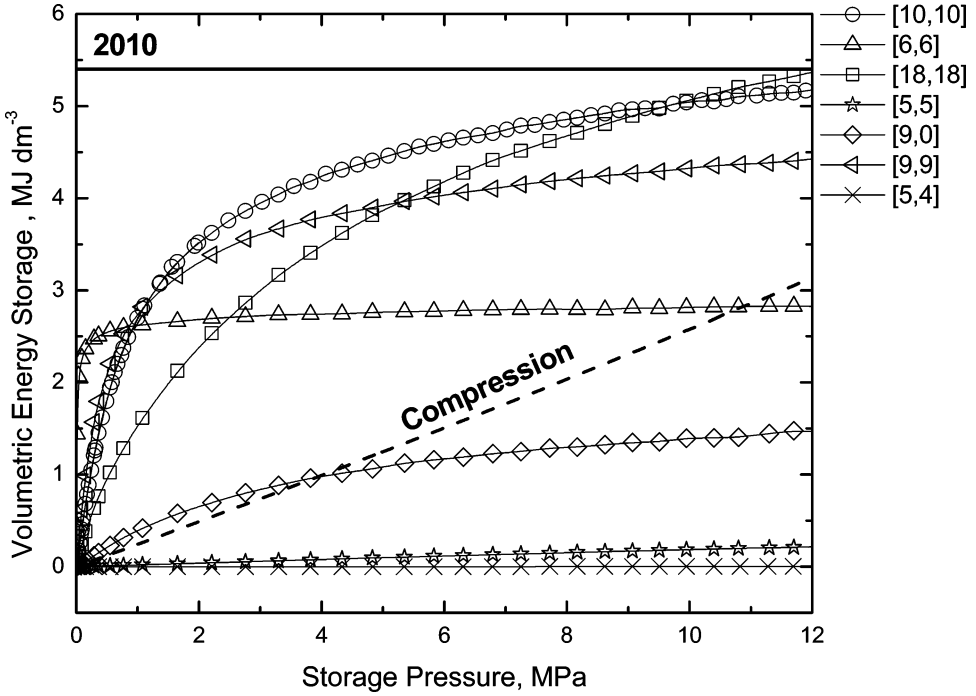

Figure 1. Pressure variation of stored volumetric energy of equimolar mixture of hydrogen and methane in various idealized bundles of SWNTs at 293 K. The nanotube chiral vector is defined as [*n*,*m*]. Solid line corresponds to target established by the U.S. FreedomCAR Partnership 5.4 MJ dm^{-3} by 2010.[25] Dashed line corresponds to the volumetric energy of the compressed equimolar of hydrogen and methane.

TABLE 1: Comparison of the Storage Properties of the Investigated Idealized Bundles of SWNTs and Compression Method for Equimolar Mixture of Hydrogen and Methane at 293 K

chiral vector	pore radius, Å	volumetric energy storage at 12 MPa	hydrogen content (%) at 12 MPa
[10,10]	6. 8	5.2	7.9
[6,6]	4.1	4.4	4.1
[18,18]	12.2	5.4	10.5
[5,5]	3.4	0.2	95.9
[9,0]	3.5	1.5	20.5
[9,9]	6.1	4.4	8.9
[5,4]	3.1	0.003	100.0
compression		3.2	21.6

stored volumetric energy greatly depends on the chiral vector (i.e., pore diameter) of the nanotubes forming the bundle, as seen in Figure 1 and Table 1. We see that the idealized bundle of [5,4] SWNTs is too narrow for either hydrogen or methane adsorption at considered storage conditions. The diameter of a [5,4] nanotube equals 6.2 Å. This diameter can be regarded as the threshold value below which the densification of these fluids in the idealized bundle of SWNTs is negligible. A slight increase of the pore diameter up to 6.8 Å (equivalent chiral vector [5,5]) or 7.0 Å (equivalent chiral vector [9,0]) SWNTs results in increasing the total volumetric energy, as displayed in Figure 1. However, the stored volumetric energy in these bundles is lower in comparison to simple bulk compression of the equimolar mixture of hydrogen and methane at 293 K and pressures up to 12 MPa. To better understand these results, we have computed the hydrogen content by energy in adsorbed fluid and equilibrium selectivity of methane over hydrogen, as displayed in Figures 2 and 3. The [5,5] SWNTs bundle behaves as a perfect molecular sieve for separation of hydrogen from methane at 293 K and the whole range of pressures investigated in the current work. Their tube diameter equals 6.8 Å, and the interstitial channels of this membrane are too small for accommodation of methane molecules. At the same conditions, the smaller hydrogen molecules can be adsorbed in the internal and interstitial channels between the nanotubes. For real SWNTs bundles we can suspect some variation of the distance between the single-walled tubes ≈(3.4,4.0) Å. Even with this variation of the intertube distance, the idealized [5,5] SWNTs bundle cannot adsorb methane. To confirm this result, we simulated the adsorption of hydrogen−methane mixture at 293 K and pressures from 0.001 Pa up to 12 MPa for different molar ratio of both fluids in the bulk phase. For the bulk methane-rich phase (methane molar ratio is 0.9, and hydrogen 0.1) the stored volumetric energy is very small (0.05 MJ dm^{-3} for storage pressure 12 MPa), as presented in the Supporting Information Figures 1S and 3S. Increasing the molar ratio of hydrogen in the bulk hydrogen−methane mixture results in enhancement of the stored volumetric energy and hydrogen content in the adsorbed phase due to adsorption of pure hydrogen, as presented in the Supporting Information Figures 1S and 3S. Summing up, membranes of this material can only adsorb hydrogen from a methane/hydrogen mixture of different composition at considered external conditions.

Further increment of the tube diameter in the idealized bundle of SWNTs up to 7.0 Å results in competitive adsorption of hydrogen and methane at considered storage conditions. The equilibrium selectivity reveals slight preferential adsorption of methane at low storage pressures (i.e., equilibrium selectivity defined by eq 11 is near 2) and no preference for hydrogen and methane at pressures greater than 7 MPa and 293 K. From all considered SWNT bundles, this one behaves closest to bulk compression, as seen in Figures 1 and 2.

On the contrary, for an idealized [6,6] SWNTs bundle (i.e., nanotube diameter is 8.2 Å) we observe that almost pure methane is adsorbed in the interior space of the nanotubes. The equilibrium selectivity of methane over hydrogen at 293 K rapidly increases to infinity for storage pressures approaching zero. Moreover, we see that the idealized bundle composed of cylindrical nanotubes with diameter equal 8.2 Å is completely filled by methane at 0.04 MPa and further compression of adsorbed methane slightly increases the volumetric stored

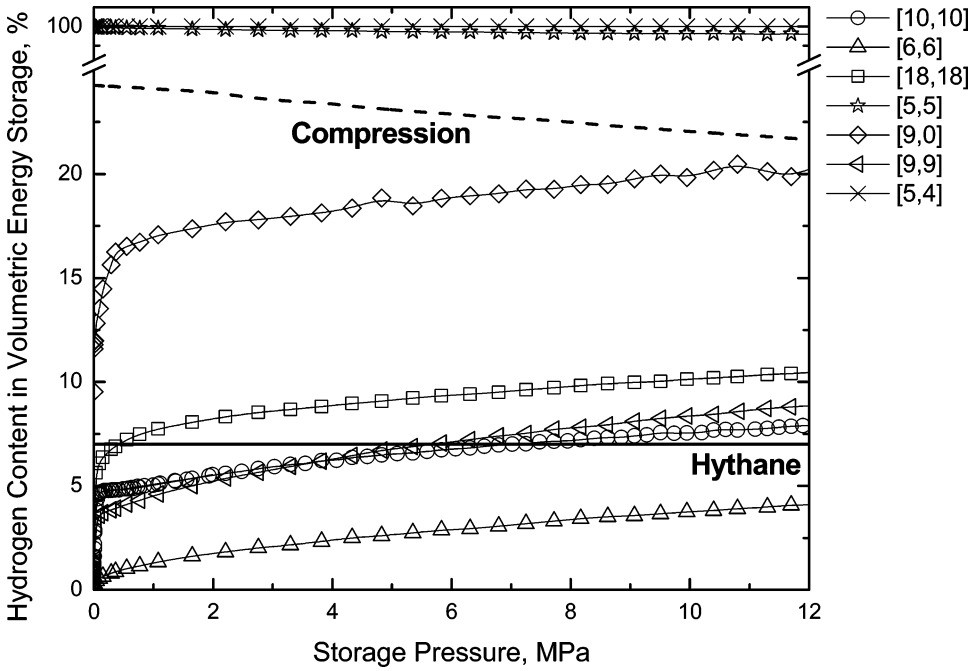

Figure 2. Content of hydrogen in stored volumetric energy of equimolar mixture of hydrogen and methane in various idealized bundles of SWNTs at 293 K. Solid line corresponds to contribution of hydrogen in hythane fuel (≈7% by energy).[61,62] Dashed line corresponds to the contribution of hydrogen to the volumetric energy of the compressed equimolar of hydrogen and methane.

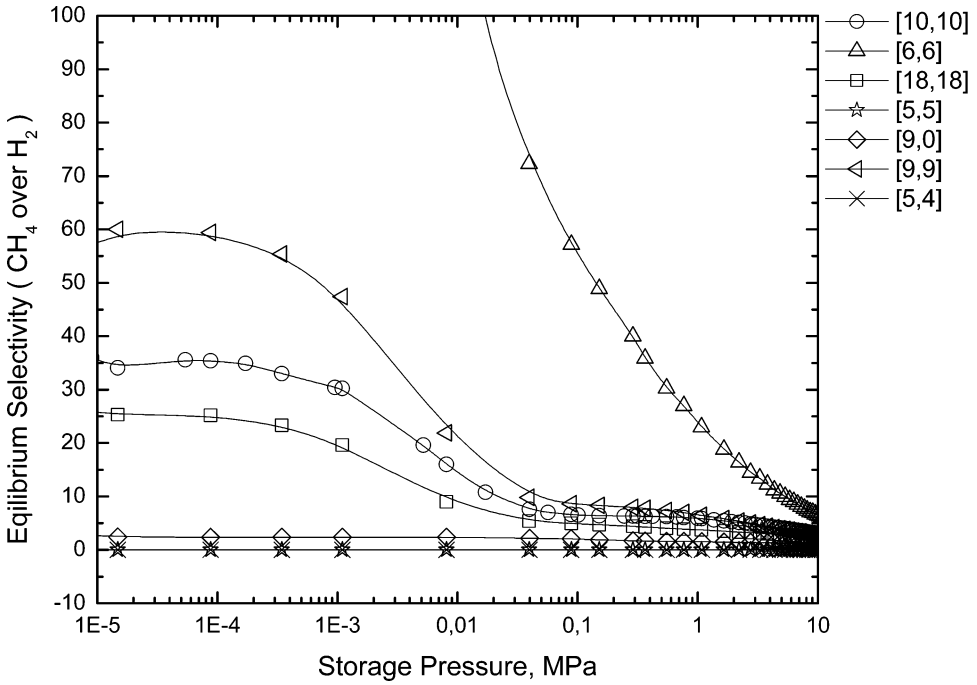

Figure 3. Pressure variation of equilibrium selectivity of methane over hydrogen in the investigated idealized bundles of SWNTs at 293 K.

energy, as displayed in Figure 1. The content of hydrogen by energy monotonically increases with storage pressure owing to adsorption of hydrogen in the interstitial channels of the [6,6] SWNTs bundle. Clearly, this leads to reduction of the equilibrium selectivity of methane over hydrogen, as seen in Figure 3. As pointed out above, for any real bundles of SWNTs we can expect variation of the intertube distance within limited range. Manipulation of the intertube distance of the interstitial channels of our idealized bundle of [6,6] SWNTs can be used for tuning the content of the adsorbed molecular hydrogen, as seen in Figures 4S−6S. We would like to underline that for reasonable intertube distance ≈3.5−3.6 Å the idealized bundle of SWNTs composed of cylindrical pores of diameter 8.2 Å seems to be attractive as a membrane for separation of methane from its mixture with molecular hydrogen at 293 K and the considered range of pressures.

Our GCMC simulations indicated that high cohesive forces cause strong compression of methane molecules in the interior space of the cylindrical nanotubes with diameter equal to 8.2 Å, as presented in Figures 4 and 5. We observe long-range order in compressed methane molecules with average intermolecular distance lower than the ones characteristic for methane bulk liquid at 111.5 K, as displayed in Figure 4.[64] Due to some degree of freedom in the interior space of these carbon nanotubes, methane molecules form a quasi-one-dimensional crystal at thermodynamic equilibrium at 293 K. The walls of these

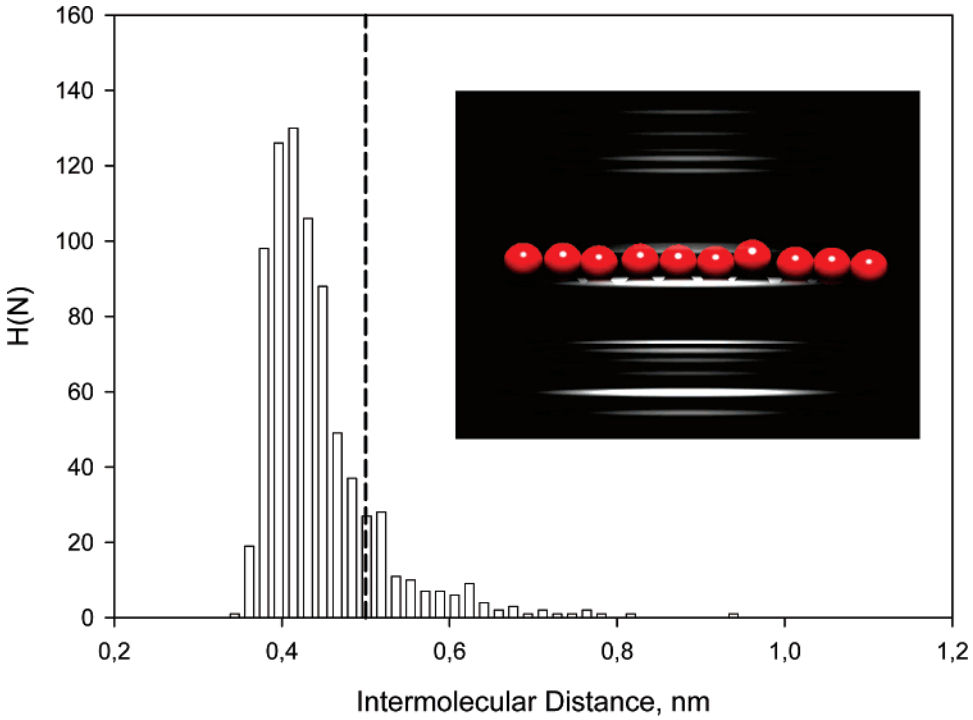

Figure 4. Histogram of the intermolecular distance between the methane molecules compressed in the interior tubes of the idealized bundle of [6,6] SWNTs at 293 K. Dashed line corresponds to the average intermolecular distance between the methane molecules in the bulk liquid at 111.5 K.[64]

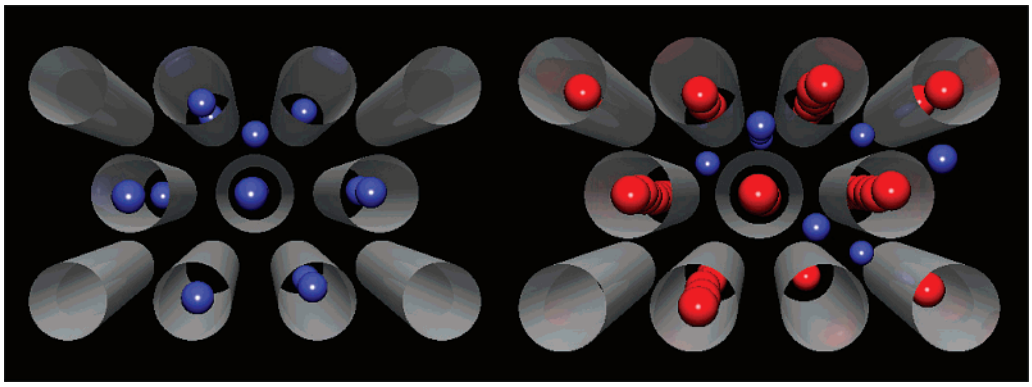

Figure 5. Equilibrium snapshot of equimolar mixture of hydrogen and methane at 293 K and 12.2 MPa in idealized bundle of [5,5] (left panel) and [6,6] (right panel) SWNTs. The intertube distance is 4 Å.

nanotubes pretend spontaneous fluctuations (i.e., spontaneous waves of compressed methane molecules) of adsorbed methane molecules that should cause rapid destruction of quasi-one-dimensional crystal structure. Increasing the molar ratio of methane in the bulk hydrogen−methane mixture shifts the pressure for the quasi-one-dimensional crystal formation to lower values.

As for methane, molecular hydrogen forms a quasi one-dimensional crystal in the interior of [5,5] SWNTs bundles, as seen in Figure 5 and Supporting Information Figure 3S. Due to higher thermal motions of hydrogen molecules in comparison to methane ones at 293 K (i.e., weaker solid−fluid interaction of hydrogen) the formation of quasi-one-dimensional hydrogen in the interior space of these SWNTs needed higher pressure of equimolar mixture of hydrogen−methane or higher partial pressure of hydrogen in this mixture. Our quasi-one-dimensional hydrogen crystal formed in the interior space of the carbon nanotubes with pore diameter equal to 6.8 Å is stable at 293 K. However, the key problem is the length of the hydrogen crystal structure formed in the interior space of these nanotubes. This phenomenon may be very interesting for ballistic flow of current in nanoscale devices. One expects that the compressed molecular hydrogen rod will drastically influence the discrete states of conduction electrons bound in this carbon nanotube. Experimental investigations of flow of current with quasi-one-dimensional hydrogen crystal formed in the interior space of the [5,5] carbon nanotubes at 293 K are needed for employing these nanostructures in nanoscale devices.

The remaining investigated idealized bundles of SWNTs are characterized by wider pore diameters of the individual nanotubes, as displayed in Table 1. As one can expect, all of them preferentially adsorbed methane at lower pressures owing to higher methane−carbon binding energy in comparison to that for molecular hydrogen, as shown in Figures 1−3, 6, and 7. The high equilibrium selectivity of methane over hydrogen observed for idealized bundles of [9,9] (diameter 12.2 Å) and [10,10] (diameter 13.6 Å) SWNTs suggests that the membranes composed of these nanomaterials are promising for separation of methane from their mixture with hydrogen. Moreover, from Figures 1 and 2 we recognize that these nanomaterials are very

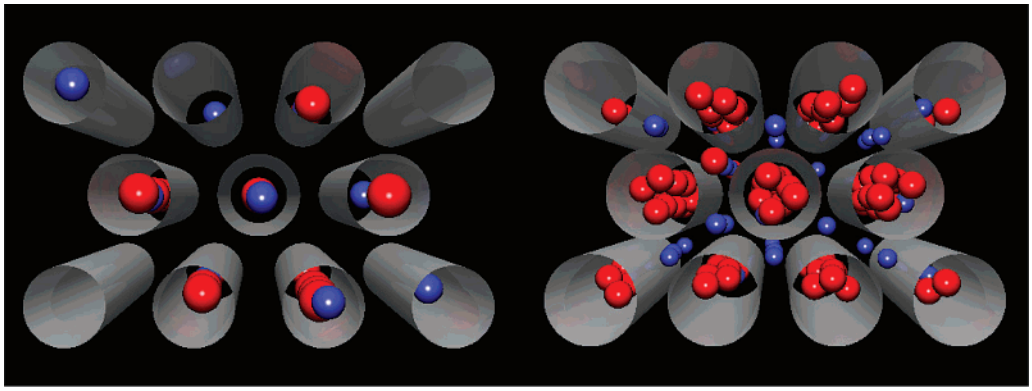

Figure 6. Equilibrium snapshot of equimolar mixture of hydrogen and methane at 293 K and 12.2 MPa in idealized bundle of [9,0] (left panel) and [9,9] (right panel) SWNTs. The intertube distance is 4 Å.

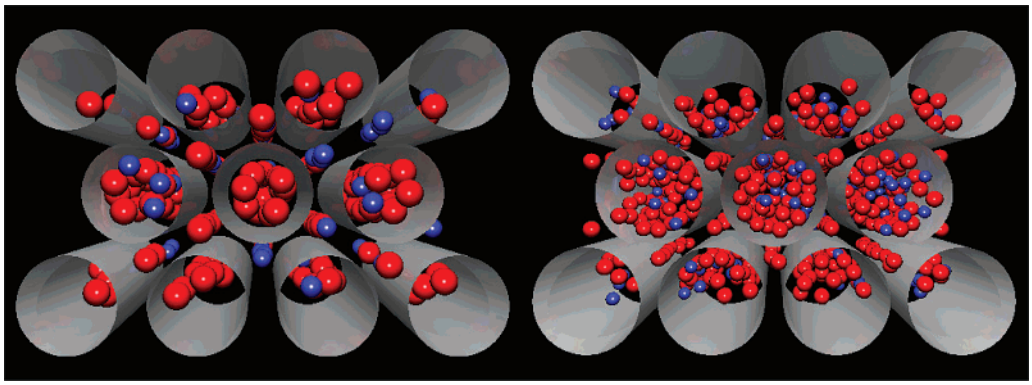

Figure 7. Equilibrium snapshot of equimolar mixture of hydrogen and methane at 293 K and 12.2 MPa in idealized bundle of [10,10] (left panel) and [18,18] (right panel) SWNTs. The intertube distance is 4 Å.

promising for storage of hythane fuel since both idealized bundles of SWNTs preferentially adsorbed methane with additional small content of hydrogen. Clearly, manipulation of bulk-phase composition of methane and hydrogen can be used for tuning the hydrogen content in the adsorbed phase. The advantages of tubular carbon nanostructures (i.e., SWNHs, SWNTs, and others) over ordinary activated carbons are well-defined pore structure and purity.

Interestingly, SWNTs characterized by pore diameter equal to 12.2 Å primarily adsorbed molecular hydrogen in the interstitial channels, as seen in Figure 6. At the same time, methane filled the internal carbon pores and was highly compressed. It is worth stressing that produced SWNTs are originally closed. As a result, the membrane composed of these SWNTs with closed internal cylindrical pores seems to be an interesting candidate for sieving of hydrogen form their mixture with methane at considered storage conditions. Increase of tube diameter above 24.4 Å (i.e., [18,18] nanotube) causes reduction of both volumetric energy storage and selectivity of methane over hydrogen and increase of the hydrogen content in adsorbed phase, as displayed in Figures 1, 3, and 7. As a result, the membranes composed with SWNTs with greater pore diameter are less efficient.

Conclusions

We have used Grand Canonical Monte Carlo simulations for modeling hydrogen and methane mixture storage and separation in selected idealized bundles of SWNTs at 293 K and pressures ranging from 0.001 Pa up to 12 MPa. We have found that the value of the stored volumetric energy and the equilibrium selectivity greatly depends on the chiral vector (i.e., pore diameter) of the nanotubes composing the idealized bundle. The [5,4] SWNTs bundle can be regarded as a threshold value below which the densification of hydrogen or methane is negligible. Our simulations indicated that bundles with wider tube diameter (i.e., 12.2, 13.6, 24.4 Å) seem to be plausible nanomaterials for hythane storage and separation of methane from its mixture with hydrogen at 293 K and low pressures. These materials efficiently adsorb methane at considered storage conditions. As a result, they greatly enhance volumetric energy storage in comparison to the classical compression method. On the other hand SWNTs with pore diameter greater than 24.4 Å (i.e., [18,18] nanotube) are less efficient for both on-board vehicle energy storage and separation of hydrogen−methane mixture at 293 K and pressures up to 12 MPa. The idealized bundle of [6,6] SWNTs is the most efficient room-temperature filter studied for separation of methane from its mixture with hydrogen. At equilibrium, in the interior spaces of these nanotubes adsorbed/compressed methane formed a quasi-one-dimensional crystal with average intermolecular distance lower than the one for bulk liquid methane at 111.5 K. On the other hand, for smaller pore diameter of 6.8 Å the hydrogen can enter into the tubes and methane remaining in bulk. We found that in the interior of [5,5] nanotubes adsorbed/compressed hydrogen forms a quasi-one-dimensional crystal.

Supporting Information Available: Graphs of the bulk hydrogen and methane mixture composition at 293 K showing the volumetric energy stored and the hydrogen content in the idealized bundles of [5,5] SWNTs, impact of intertube distance on the volumetric energy stored, and hydrogen content in an idealized bundle of [6,6] SWNTs and snapshots of hydrogen and methane mixtures for different molar ratios of hydrogen and methane in bulk phases. This material is available free of charge via the Internet at http://pubs.acs.org.

References and Notes

(1) Gadd, G. E.; Blackford, M.; Moricca, S.; Webb, N.; Evans, P. J.; Smith, A. M.; Jacobsen, G.; Leung, S.; Day, A.; Hua, Q. *Science* **1997**, *277*, 933.

(2) Schlapbach, L.; Züttel, A. *Nature* **2005**, *414*, 353.

(3) Bhatia, S. K.; Myers, A. L. *Langmuir* **2006**, *22*, 1688.

(4) Suenaga, K.; Okazaki, T.; Wang, C. R.; Bandow, S.; Shinohara, H.; Iijima, S. *Phys. Rev. Lett.* **2003**, *90*, 055506.

(5) Kowalczyk, P.; Solarz, L.; Do, D. D.; Samborski, A.; MacElroy, J. M. D. *Langmuir* **2006**, *22*, 9035.

(6) Gogotsi, Y.; Dash, R. K.; Yushin, G.; Yildrim, T.; Laudisio, G.; Fischer, J. E. *J. Am. Chem. Soc.* **2005**, *127*, 16006.

(7) Hirscher, M.; Becher, M. *J. Nanosci. Nanotechnol.* **2003**, *3*, 3.

(8) Dillon, A. C.; Heben, M. J. *Appl. Phys. A* **2001**, *72*, 133.

(9) Tanaka, H.; Kanoh, H.; Yudasaka, M.; Iijima, S.; Kaneko, K. *J. Am. Chem. Soc.* **2005**, *127*, 7511.

(10) Guay, P.; Stansfield, B. L.; Rochefort, A. *Carbon* **2004**, *42*, 2187.

(11) Bhatia, S. K.; Tran, K.; Nguyen, T. X.; Nicholson, D. *Langmuir* **2004**, *26*, 9612.

(12) Miyamoto, J.; Hattori, Y.; Noguchi, D.; Tanaka, H.; Ohba, T.; Utsumi, S.; Kanoh, H.; Kim, Y. A.; Muramatsu, H.; Hayashi, H.; Endo, M.; Kaneko, K. *J. Am. Chem. Soc.* **2006**, *128*, 12636.

(13) Wang, Q.; Challa, S. R.; Sholl, D. S.; Johnson, J. K. *Phys. Rev. Lett.* **1999**, *82*, 956.

(14) Kowalczyk, P.; Bhatia, S. K. *J. Phys. Chem. B.* **2006**, *110*, 23770.

(15) Kurniawan, Y.; Bhatia, S. K.; Rudolph, V. *AIChE* **2006**, *52*, 957.

(16) Jiang, J.; Sandler, S. I. *Langmuir* **2003**, *19*, 5936.

(17) Arora, G.; Sandler, S. I. *J Chem. Phys.* **2005**, *123*, 044705.

(18) Challa, S. R.; Sholl, D. S.; Johnson, J. K. *Phys. Rev. B* **2001**, *63*, 245419.

(19) Beenakker, J. J. M.; Borman, V. D.; Krylov, S. Yu. *Chem. Phys. Lett.* **1995**, *232*, 379.

(20) Gubbins, K. E.; Quirke, N. In *Molecular Simulation and Industrial Applications: Methods, Examples and Prospects*; Gubbins, K. E., Quirke, N., Eds.; Gordon and Breach Science Publishers: Amsterdam, 1996.

(21) Ciach, A. *Prog. Colloid Polym. Sci.* **2004**, *129*, 40.

(22) Evans, R. D. in *Fundaments of Inhomogeneous Fluids*; Henderson, D., Ed.; Marcel Dekker, Inc.: New York, 1992.

(23) Hansen, J. P.; McDonald, I. R. *Theory of Simple Liquids*; Academic Press: London, 1990.

(24) Saito, R.; Dresselhaus, G.; Dresselhaus, M. S. *Physical Properties of Carbon Nanotubes*; Imperial College Press: London, 1998.

(25) Dell, R. M.; Rand, D. A. J. *Clean Energy*; The Royal Society of Chemistry: Cambridge, 2004.

(26) Takagi, H.; Hatori, H.; Soneda, Y.; Yoshizawa, N.; Yamada, Y. *Mater. Sci. Eng. B* **2004**, *108*, 143.

(27) Iijima, S.; Yudasaka, M.; Yamada, R.; Bandow, S.; Suenaga, K.; Kokai, F. *Chem. Phys. Lett.* **1999**, *309*, 165.

(28) Holt, J. K.; Park, H. G.; Wang, V.; Stadermann, M.; Artyukhin, A. B.; Grigoropoulos, C. P.; Noy, A.; Bakajin, O. *Science* **2006**, *312*, 1034.

(29) Sholl, D. S.; Johnson, J. K. *Science* **2006**, *312*, 1003.

(30) Gordillo, M. C.; Boronat, J.; Casulleras, *Phys. Rev. B* **2000**, *61*, R878.

(31) Gordillo, M. C.; Boronat, J.; Casulleras, *Phys. Rev. B* **2002**, *65*, 014503.

(32) Gordillo, M. C.; Marti, J. *Chem. Phys. Lett.* **2001**, *341*, 250.

(33) Michel, K. H.; Verberck, B.; Nikolaev, A. V. *Phys. Rev. Lett.* **2005**, *95*, 185506.

(34) Britz, D. A.; Khlobystov, A. N. *Chem. Soc. Rev.* **2006**, *35*, 637.

(35) Chen, H.; Johnson, J. K.; Sholl, D. S. *J. Phys. Chem. B* **2006**, *110*, 1971.

(36) Jiang, J.; Sandler, S. I.; Smit, B. *Nano Lett.* **2004**, *4*, 241.

(37) *Coalbed Methane: Scientific, Environmental and Economic Evaluation*; Mastalerz, M., Glikson, M. V., Golding, S. D., Eds.; Kluwer: Dordrecht, 1999.

(38) Hoogers, G. *Fuel Cell Technology Handbook*; CRC: Oxford, 2002.

(39) Hu, Y. H.; Yu, N. Y.; Ruckenstein, E. *Ind. Eng. Chem. Res.* **2004**, *43*, 4174.

(40) Alapati, S. V.; Johnson, J. K.; Sholl, D. S. *J. Phys. Chem. B* **2006**, *110*, 8769.

(41) Lee, H.; Lee, J-W.; Kim, D. Y.; Park, J.; Seo, Y-T.; Zeng, H.; Moudrakovski, I. L.; Ratcliffe, C. I.; Ripmeester, J. A. *Nature* **2005**, *434*, 743.

(42) Kowalczyk, P.; Tanaka, H.; Hołyst, R.; Kaneko, K.; Ohmori, T.; Miyamoto, J. *J. Phys. Chem. B* **2005**, *109*, 17174.

(43) Ohba, T.; Kanoh, H.; Yudasaka, M.; Iijima, S.; Kaneko, K. *J. Phys. Chem. B* **2005**, *109*, 8659.

(44) Tanaka, H.; Fan, J.; Kanoh, H.; Yudasaka, Yudasaka.; Iijima, S.; Kaneko, K. *Mol. Simul.* **2005**, *31*, 465.

(45) Urita, K.; Seki, S.; Utsumi, S.; Noguchi, D.; Kanoh, H.; Tanaka, H.; Hattori, Y.; Ochiai, Y.; Aoki, N.; Yudasaka, M.; Iijima, S.; Kaneko, K. *Nano Lett.* **2006**, *6*, 1325.

(46) Yumura, T.; Sato, Y.; Suenaga, K.; Urita, K.; Iijima, S. *Nano Lett.* **2006**, *6*, 1389.

(47) Gordillo, M. C.; Brualla, L.; Fantoni, S. *Phys. Rev. B* **2004**, *70*, 245420.

(48) Sese, L. M. *Mol. Phys.* **1994**, *81*, 1297.

(49) Sese, L. M. *Mol. Phys.* **1995**, *85*, 931.

(50) Sese, L. M. *Chem. Phys. Lett.* **1997**, *266*, 130.

(51) Sese, L. M. *Mol. Phys.* **1993**, *78*, 1167.

(52) Levesque, D.; Gicquel, A.; Darkrim, F. L.; Kayiran, S. B. *J. Phys. Condens. Matter* **2002**, *14*, 9285.

(53) Allen, M. P.; Tildesley, D. J. *Computer Simulation of Liquids*; Clarendon: Oxford, 1987.

(54) Steele, W. A.; Bojan, M. *Adv. Colloid Interface Sci.* **1998**, *153*, 76−77.

(55) Gordillo, M. C. *Phys. Rev. Lett.* **2006**, *96*, 216102.

(56) Murata, K.; Kaneko, K.; Steele, W. A.; Kokai, F.; Takahashi, K.; Kasuya, D.; Hirahara, K.; Yudasaka, M.; Iijima, S. *J. Phys. Chem. B* **2001**, *105*, 10210.

(57) Bekyarova, E.; Kaneko, K.; Yudasaka, M.; Kasuya, D.; Iijima, S.; Huidobro, A.; Rodriguez-Reinoso, F. *J. Phys. Chem. B* **2003**, *107*, 4479.

(58) Feynman, R. P.; Hibbs, A. *Quantum Mechanics and Path Integrals*; McGraw-Hill: New York, 1965.

(59) Wang, Q.; Johnson, J. K. *J. Chem. Phys.* **1999**, *110*, 577.

(60) Frenkel, D.; Smit, B. *Understanding Molecular Simulation Form Algorithms To Applications*; Academic Press: London, 1996.

(61) Green Car Congress website: www.greencarcongress.com.

(62) Hythane Company website: www.hythane.com.

(63) Tan, Z.; Gubbins, K. E. *J. Phys. Chem. B* **1992**, *96*, 845.

(64) Zahn, D. *J. Phys. Chem. B* **2006**, *110*, 19601.